GROUND-BASED SUPERCOOLED LIQUID WATER MEASUREMENTS IN WINTER OROGRAPHIC CLOUDS

Mark E. Solak, Rand B. Allan and Thomas J. Henderson
Atmospherics Incorporated
Fresno, CA 93727

ABSTRACT The use of ice detectors at mountain-top sites in winter orographic weather modification projects in the western U.S. is described. Refinements in data acquisition and interpretation are presented. The superiority of ice detector analog voltage records over deice signal-only data for determination of SLW characteristics is demonstrated. It is shown that ground-based ice detector and radiometer-derived supercooled liquid water (SLW) flux estimates exhibit reasonable correspondence. Ground-based SLW flux records are used with precipitation data to produce indications of precipitation efficiency, showing orderly transitions between periods of efficiency and inefficiency within storms. Ground-based SLW flux data suggest that, in some instances, increased precipitation rates alone do not necessarily signal diminished seeding opportunity.

1. INTRODUCTION

It has long been understood that a pivotal factor in any program designed to either apply or investigate winter orographic precipitation enhancement by use of freezing nuclei is the occurrence of supercooled liquid water (SLW) within cloud systems. In recent years the role and importance of low altitude SLW in winter orographic storms has been investigated with renewed vigor. This article provides an update on use of ground-based ice accretion measurements by Atmospherics Incorporated (AI) in the western U.S. Those measurements are used to investigate some aspects of winter orographic cloud systems relating to their precipitation enhancement potential.

Continuous measurements using ice detectors at mountain-top sites for the specific purpose of investigating low altitude supercooled liquid water for weather modification program design and decision making began in California with AI's observations on Squaw Peak near Lake Tahoe. That work was conducted as part of the Sierra Cooperative Pilot Project (SCPP), a winter precipitation enhancement research program funded by the Bureau of Reclamation. The initial methodology and findings have been reported in Henderson and Solak (1983) and Solak et al (1984). Those results, combined with microwave radiometer measurements in the same region (e.g., in Snider and Rottner, 1982), influenced a shift in the focus of SCPP research from primarily postfrontal convection to the more stratiform and widespread cloud types.

Earlier SCPP SLW investigations, based primarily on airborne observations and measurements, had suggested that very little SLW occurred in the stratiform cloud types. However, it became clear that the airborne investigations in stratiform situations were often severely limited by terrain-avoidance constraints on low altitude flight operations, yielding an incomplete assessment of SLW occurrence. In contrast, the mountain-top measurements supported earlier conventional wisdom and long-standing operational assumptions that significant amounts of SLW are commonly produced and often concentrated at low altitudes. That view arose from observations of significant rime ice accumulation on vegetation and structures in high terrain. It has been strengthened by seeding aircraft observations over other portions of the Sierra, and by airborne research measurements over and near the SCPP study area (Lamb et al, 1976).

Those early Sierra ground-level SLW studies highlighted the important practical factor of potential weather modification yield, which is affected by cloud coverage and type and has its upper limit defined by the magnitude of the SLW occurrence (i.e., the total mass of SLW potentially available for conversion and/or accretion, per storm or per unit time). In SCPP, although some cumuli were considered to present good seeding potential, their contribution to season total precipitation was recognized as being comparatively small. In contrast, the more widespread stratiform cloud systems were known to contribute a significant proportion of seasonal precipitation. The growing evidence in SCPP of substantial SLW occurring within those stratiform cloud systems made them increasingly attractive as potential seeding candidates.

Recent weather modification research, largely in the western states, has shed additional light on the occurrence and character of low altitude SLW, as well as at other levels, and its implications relative to weather modification potential, e.g., Sassen (1985) in Utah, Rauber et al (1986) in northern Colorado and Thompson and Super (1987) over Colorado's Grand Mesa. These and other recent findings have been based on measurements using research systems such as microwave radiometers, short wavelength radars and lidars. One of the goals of the work reported here is to demonstrate the utility of the comparatively simple mountain-top SLW measurement system to (1) provide useful operational seeding decision making guidance and (2) augment full cloud depth SLW measurements in research programs.

2. OBSERVATION SYSTEM

The prototype system used at the Squaw Peak site in California, described in detail in Henderson and Solak (1983), consisted basically of

an ice detector, heated cup and vane wind system, temperature sensor, back-up power system, and chart recorders. Some modifications were later incorporated, most notably inclusion of a heated orthogonal anemometer which provides high quality wind data with great reliability in icing environments. Since 1987 the SLW system has included onsite computerized data acquisition, producing high quality data at 5-min intervals, averaged from 5-sec sampling. The chart recorders have been retained to provide analog ice accretion records and to serve as backup to the computerized acquisition.

The key component of the SLW systems has been the Rosemount ice detector model 871FA, an electro-mechanical device which automatically deices and transmits a signal when a specified amount of ice has accreted onto its sensing element. After the deicing (heat) cycle, the detector cools and returns to sensing status in approximately 60 seconds. The model 871FA detector also provides a continuous analog output of the sensing probe oscillation frequency which corresponds to the instantaneous sensor ice load. Another model ice detector, the Rosemount 872B, has also been evaluated for possible incorporation into operational systems. The model 872B heats for 90 seconds, and requires approximately 4-5 minutes to cool sufficiently after each heat cycle to again accumulate rime ice. The 872B currently provides a deice signal only. Records from the ice detector(s) are used in conjunction with wind measurements to produce estimates of average SLW concentration at appropriate time intervals.

3. DATA ASPECTS

Our initial data interpretations, detailed in Henderson and Solak (1983), involved a "trip counting" method which is based on the ice detector's deice cycles. Note: the terms "trip" and "deice cycle" are used interchangeably, and refer to the point in time when the ice accumulation triggers the detector's heaters and a discrete deice signal is provided for the 6-7 second heat duration of the 871FA. Using each deice cycle to define an averaging interval, or by counting deice events within fixed time intervals, mean values of wind velocity were used with the cross-section area of the detector's sensing element to estimate sample volume (i.e., the volume swept out by the probe). The known ice mass (trip) accumulations and sample volume estimates were then used to produce crude estimates of SLW concentration in the air passing the measurement site. Only storms producing sufficient ice accretion on the probe to trigger its deicing heaters were analyzed. This method is still used by some investigators. Some important limitations of this basic method are described in part 4 of this article.

Onsite observations of the ice detector's performance in a variety of icing conditions have led to adjustments to our data reduction and SLW parameter calculation methods. For example, observations of the detector's very low sensing threshold, combined with its ability to accurately indicate small scale variability during ice accretion events, has enabled a shift from the deice signal-only data to the oscillation frequency analog output for accurate determination of ice accretion values. Further, the effects of residual melt (not totally shed after deicing) which can occur in light wind situations are now eliminated during data reduction. These adjustments have improved the accuracy and utility of the observations. The key refinements and additions in data reduction and SLW calculations are listed below.

- Analog ice detector oscillation frequency records from the model 871FA are manually reduced to determine ice accretion mass values. This allows identification and analysis of rime ice accumulation periods of "sub-trip" magnitude which are not documented in "trip-only" output. The data reduction interval can then be tailored to specific project requirements. Part 4 of this article describes the output differences in more detail.
- Effects of residual melt drops on sensing element downward operations (after heat cycles) are identified in analog traces and excluded from calculations.
- Ice detector model 871FA 60 sec off-duty (heat, cooldown) periods are eliminated from in sample volume estimates.
- First-order adjustments for estimated droplet collection efficiency are applied to accumulation amounts, based on laminar flow equations originally develop by Ranz and Wong (1952).
- SLW flux estimates are routinely developed for assessing event magnitude and comparison with other SLW observations.

4. ICE DETECTOR OUTPUT COMPARISONS AND USES

Our investigations have involved the Rosemount model 871FA and 872B ice detectors. Both employ the same operating principle and sensing element configuration. However, having been designed for distinctly different uses, their standard outputs differ. The model 871FA was developed for the aviation industry and provides an analog output corresponding to rime loading on its sensing element, as well as a 6-7 sec deice signal when a preset rime load threshold has accumulated and the instrument's deicing heater is triggered. Thus, it senses and indicates. In contrast, the more recent model 872B was designed for use as a warning device for fixed structures and produces only a deice signal after significant atmospheric icing has occurred. Those output differences must be carefully considered when using the data to assess atmospheric conditions.

Our initial data interpretations were based on the "trip counting" (deice signal) method used in recent years by a few investigators. But, field observations and data comparisons (detailed below) have provided convincing evidence that using the analog (sensing) output is superior for research applications. Consequently, all results in this article are based on manually reduced analog records of ice accretion.

To illustrate the differences between the two probe models' output, a simulated chart section is shown in Figure 1. It depicts the combined analog and trip signal provided by the 871FA detector as

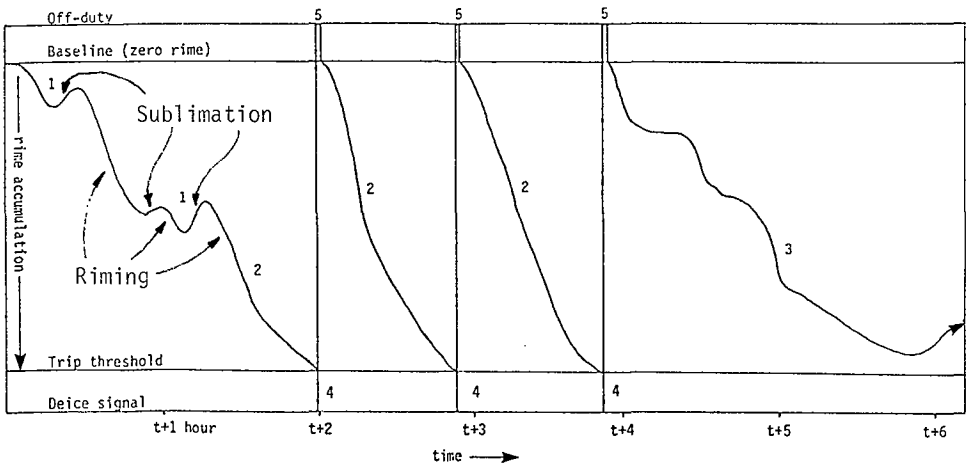

Figure 1. Example chart record of combined analog sensing (rime ice load) and deice "trip" signal output from the model 871FA ice detectors used in ground-based investigations. The trace segments are numbered for reference to text discussion.

routinely used in our field work. The 872B probe output, in its currently available configuration, would consist of the three deice trips only, with no indication of accretion rates or character. Features commonly seen in analog traces from ground-based observations are shown in Figure 1.

During storm onset the initial accumulation of rime ice on the sensor commonly occurs over a period of 2-3 or more hours before the first instrument deice cycle. The duration of this initial accumulation period is influenced by the LWC and wind velocity (i.e., the SLW flux), the preset trip threshold value and the continuity of the initial probe riming during storm onset. Interspersed riming and sublimation periods are commonly noted in analog traces prior to the first detector deicing cycle because cloud conditions fluctuate during storm onset. Prior to the first deice event in Figure 1 (chart section 4 at t+2h), 20% more actual accretion occurred than the "trip-only" output would have indicated. Rime accumulation leading to the next two trips (near t+3 and t+4), is much more uniform. No significant interspersed sublimation is indicated in the chart sections labeled "2" between t+2 and t+4, and each trip represents a true ice accumulation. However, after the third trip (near t+4) chart section 3 shows additional accretion from t+4 through t+6 that would not be indicated in the trip-only output because the deice threshold was not reached. This additional accretion, not documented in the "trip only" records, constitutes nearly 25% of the total occurring in the overall example.

In viewing the analog trace example, several drawbacks to using trip-only (standard 872B) output become apparent.

1)The 872B cannot accurately indicate the start or end of probe riming events. In contrast, the 871FA continuous analog output provides those times unambiguously.

2) The 872B cannot indicate accumulations of rime ice less than its deice threshold value. Many ice accretion events are simply not documented in trip-only data.

3) The 872B cannot accurately indicate rime accumulations when interspersed sublimation/riming periods occur.

4) The fact that the 872B data consist of "trip" points only, with no indication of the character of the ice accumulation period, forces an analyst to assume uniform conditions between instrument deicing cycles. The elapsed time between trips can vary widely, and during low magnitude icing occurrences the resultant averaging periods can be unacceptably long. The 871FA analog records capture fine-scale ice accretion rate variability and allow data reduction at uniform intervals tailored to the specific application.

5. FINDINGS

Strategically sited ground-based SLW observations can be used to address a number of practical questions related to project design and operations. Data obtained within the Utah/NOAA cooperative weather modification research program are used to address the factors of (a) accurately identifying the start and end of SLW occurrences at low altitudes, (b) determining the storm-by-storm contribution to seasonal low altitude SLW flux, (c) characterizing site winds during SLW occurrences, (d) determining temperature characteristics during those occurrences, (e) investigating relationships between SLW and precipitation and (f) assessing detector and radiometer data relationships.

The SLW system in Utah was located on an exposed ridge at 2978 m (9768') elevation approximately 3 km west of the crest of the Tushar Range in southwestern Utah (see Figure 2). The Tushars are oriented primarily north-south, rising from an 1800 m valley floor about 4 km east of Beaver to a ridgeline ranging from 3000-3700 m elevation about 20 km east. Near the SLW site the crestline averages about 3400 m. In 1987 the Utah/NOAA field operations documented 11 storms during the six-week period of 01 February through 15 March. Those 11 storms are listed in Table 1.

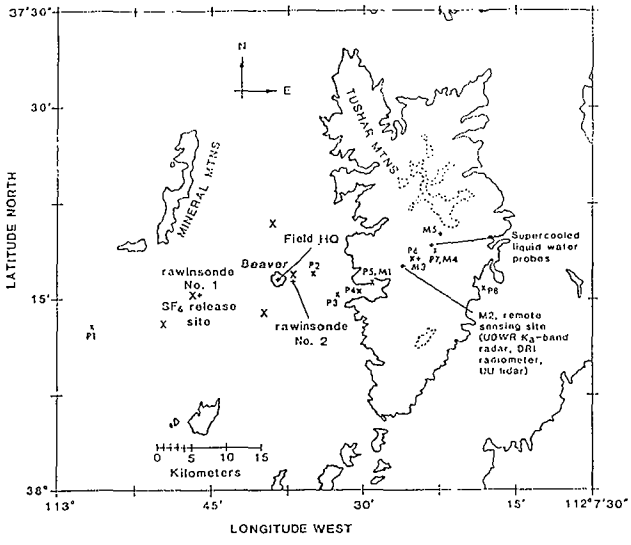

Figure 2. Locations of the instrumentation in the 1987 Utah/NOAA field research program. Symbols P1, P2, . . . indicate sites of surface precipitation gages. Symbols M1, M2, . . . indicate sites of surface precipitation microphysics observations. Large unlabeled symbols X show sites of mechanical weather stations. Contours of terrain are at 2438 m MSL (solid line) and at 3353 m MSL (dashed line).

TABLE 1. Utah/NOAA 1987 STORM periods

STORM	Date	Start Time (MST)	Date	End Time (MST)	Dur(h)
1	03 Feb 87	1300	04 Feb 87	0300	14.0
2	10 Feb 87	0730	10 Feb 87	1700	9.5
3	11 Feb 87	1500	12 Feb 87	1300	22.0
4	13 Feb 87	1500	14 Feb 87	1100	20.0
5	15 Feb 87	1600	16 Feb 87	1400	22.0
6	18 Feb 87	1400	18 Feb 87	1940	5.7
7	23 Feb 87	1000	25 Feb 87	2300	61.0
8	07 Mar 87	0800	07 Mar 87	2000	12.0
9	08 Mar 87	0500	08 Mar 87	2400	19.0
10	13 Mar 87	1330	13 Mar 87	1800	4.5
11	14 Mar 87	2300	15 Mar 87	2120	22.3
				Total:	212.0

A. Ice Detector (Model) Comparisons

Documentation of the true onset, end and character of SLW occurrences is of obvious value in operations and research applications. The Utah observations in 1987 marked our first comparisons of model 872B (trip-only) and model 871FA (analog) output from collocated detectors under field conditions. Those field comparisons, using 871FA data as a standard because of its analog output, confirmed the significant differences illustrated in the example (Figure 1) presented earlier in this article. Onsite observer's notes have verified the 871FA's low sensing threshold and the ability of its analog output to document small-scale variability. Table 2 presents the durations and magnitudes of atmospheric icing events as indicated by the two detector models during the Utah study. Durations for the 872B represent the full elapsed time between the first and last instrument trips, whereas the 871FA durations are sums of non-zero 5-minute icing periods. The SLW mass values in Table 2 were determined using the detector total ice accretion mass measurements. Those measured ice accretion amounts have been extrapolated to represent the mass of SLW passing through a window 1 meter square to facilitate comparison with other systems' data.

TABLE 2. Comparison of 871FA and 872B icing probes using 1987 season Utah/NOAA riming data

STORM	Hrs of indicated riming 872B	Hrs of indicated riming 871FA	Total ice mass ($kg\ m^{-2}$) 872B	Total ice mass ($kg\ m^{-2}$) 871FA
1	0	4.3	0	0.676
2	0	0.9	0	0.446
3	4.8	4.6	2.232	2.827
4	4.8	11.9	13.950	15.755
5	0	0.7	0	0.050
6	0	1.0	0	0.081
7	0	4.5	0	0.595
8	0	0.9	0	0.136
9	1.4	3.6	1.674	1.978
10	0	0.3	0	0.019
11	0	2.3	0	0.453
	11.0	35.0	17.856	23.016

As shown in Table 2, the 872B output indicated the presence of SLW in only three storms, although some SLW was measured in all eleven storms by the collocated 871FA. During those three storms, the 872B reported 55% of the cumulative duration and 87% of the total ice mass measured by the 871FA. Over the full season, the 872B reported 31% of the cumulative riming duration and 78% of the total ice mass. Further, STORM 3 illustrates a duration-related problem inherent in the assumptions required when using trip-only output. In that case the 872B duration is greater than that reported by the 871FA.

B. Storm Contribution to Season Total SLW Mass

SLW mass and its flux are measurements that can be used in a basic way to estimate the upper limits of seeding potential in precipitation augmentation efforts. This practical concept is important, even if used only as a coarse indicator as input to a number of weather modification considerations, such as:

- assessment of overall augmentation potential during project design,
- determination of the distribution of SLW occurrences and their relative magnitudes over a measurement period,
- developing subsequent engineers' estimates of operational levels of effort and attendant costs, and
- day-to-day operations seeding decision making, if available real-time

Using Utah/NOAA ice detector data, total SLW mass values for each of the 11 STORMS (STORMS = broadly inclusive analysis periods which encompass the early onset through dissipation phases of precipitation events) investigated during that project's 1987 field period were calculated using ground-based ice accretion data. Those values are presented in Figure 3 as a ranked cumulative distribution.

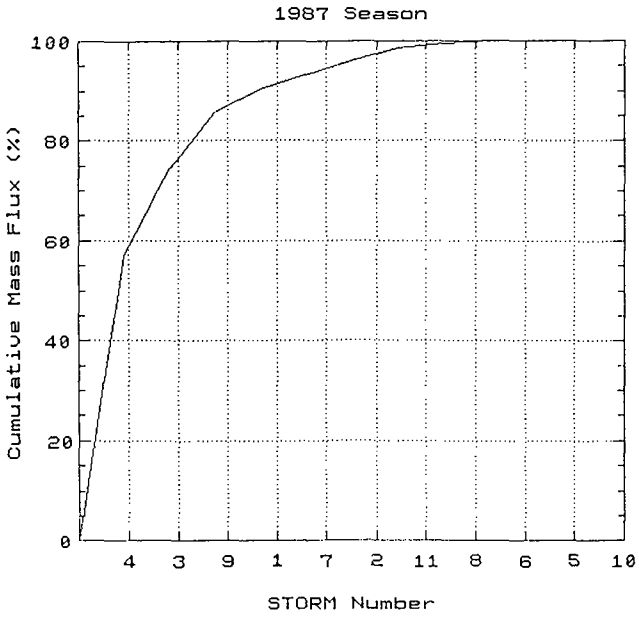

Figure 3. Cumulative SLW mass flux, 1987 season, by STORM.

It can be seen in Figure 3 that although some SLW was detected during each STORM, a small number of events contributed a large proportion of the season total amount. For example, STORMS 4, 3 and 9 produced over 85% of the total ice mass measured at the ground-based site. However, their combined duration occupied only 29% of the total season STORM duration. As an extreme example, STORM 4 alone produced well over half the season total, most of which occurred during a 7 hour period. This characteristic is consistent with indications in radiometer data from the 1985 season in Utah; Rogers et al (1986) reported that two STORMS had produced approximately 70% of the season's total liquid water flux, and that one 30 hour period had contributed nearly 50% of the season's total.

The information shown in Figure 3 and the earlier findings of Rogers et al (1986) indicate the importance of continuously monitoring the magnitude of SLW and its flux. It appears that effective precipitation enhancement research and operations must be able to identify, assess and properly respond to the comparatively few dominant events which contain the large quantities of SLW. This would be of increased importance if resources were limited.

C. SLW Versus Site Wind Characteristics

1987 Utah data during probe riming events were assessed to characterize site wind relationships with SLW content and flux. Figure 4 compares all full season non-zero SLW content and flux occurrences with wind direction at 5-min intervals.

Unadjusted SLW content is estimated using the simple expression,

$$LWC = M_t/V_s$$

where M_t is the measured ice mass (g) and V_s, the volume of air swept out by the probe, is the product of the mean wind velocity (m s^{-1}), the duration of the detector on-line period (s) and the probe cross-section (m^2). Those values are then adjusted for estimated probe collection efficiency using equations adapted from Ranz and Wong (1952). The now-computerized calculations account for the inverse relationship of collection efficiency to sensor diameter and temperature, and its direct relationship with droplet size and velocity. Average values of wind velocity and temperature are input, along with the probe diameter and, in the absence of measured droplet size spectra, an assumed 12 micron median droplet diameter. Using the indicated collection efficiency, the appropriate adjustment is then applied to each SLW value. The adjusted values are used in this article. SLW flux per unit time, in this case expressed as g m^{-2} s^{-1}, is obtained using,

$$Flux = M_t/(C*D_s)$$

where C is the probe cross-section (m^{-2}) and D_s is the sample duration in seconds.

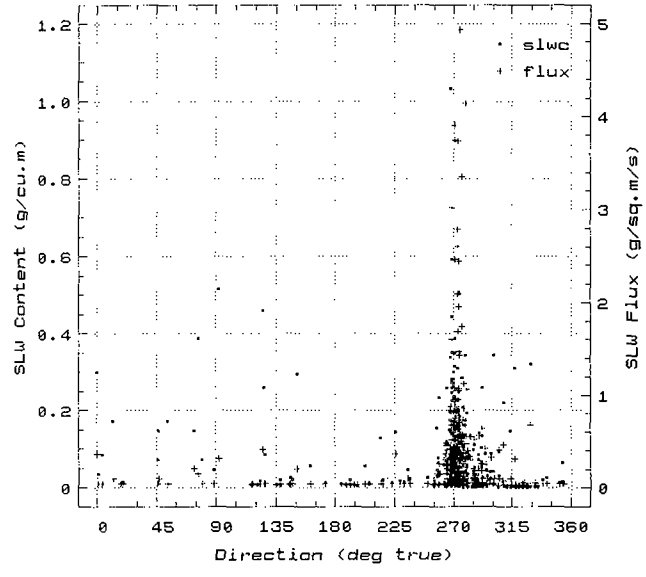

Figure 4. SLW content and flux vs. wind direction during 1987 full season combined probe riming events, 5-min averages.

The prominence of near-surface flow in the sector 260-290 during probe riming occurrences is clearly seen in Figure 4, and reflects terrain effects to a degree. However, although SLW content is seen to be somewhat a function of wind direction, SLW flux shows a much stronger wind direction dependence. Westerly flow is essentially barrier-normal to the Tushar Range which is oriented basically north-south. These data suggest that orographic lift is important in production of SLW at low altitudes.

Figure 5 compares 5-min interval SLW content and flux with wind velocity, and sheds additional light on the wind regimes which produce and enhance SLW of potential weather modification significance (i.e., comparatively large amounts for conversion to ice crystals). A weak inverse relationship (r = -.21) between SLW content and

velocity can be seen. However, SLW flux exhibits a positive and somewhat stronger relationship (r = .36), providing additional evidence of the importance of flow with a strong orographic component in SLW production.

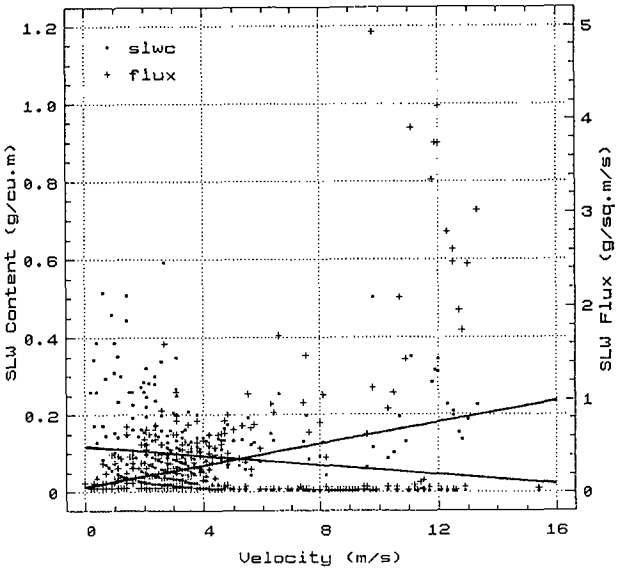

Figure 5. Regression of SLW content and flux with site wind velocity during 1987 full season combined probe riming events, 5-min averages.

D. SLW Versus Temperature

Full season SLW content and flux values, averaged for 5-min intervals, were compared with temperature data at the SLW site. Those data are shown in Figure 6. SLW was observed at temperatures as cold as -13C. Two distinct maxima in SLW content were found, from -2 to -3C and from -7 to -8C. The flux data show the same maxima, but only weakly from -7 to -8C. Inverse relationships between SLW content and site temperature were found; i.e., lower SLW content and flux values occurred generally at colder temperatures. The SLW content indication is consistent with the hypothesis put forward by Grant and Kahan (1974), that warmer orographic clouds should exhibit higher LWC values than colder orographic clouds. They reason that the higher LWC values are to be expected due to fewer snow crystals to utilize the SLW, and the greater water vapor holding capacity of warmer air. A similar inverse relationship between SLW content and temperature was shown in mountain top measurements in Colorado by Hindman (1986). The large flux values from -2 to -3C reflect the dominance of STORM 87-4 which produced over half the total season SLW mass at the detector site.

E. Relationship Between SLW and Precipitation

The relationship between supercooled liquid water and precipitation has important weather modification implications, and was also investigated in the Utah data. A project Belfort weighing gage (P6), located in the upper watershed at 2609 m elevation 3.7 km southwest of the ice detector site, was chosen for this comparison because of the completeness of its record and its relatively high data quality (locations shown in Figure 2).

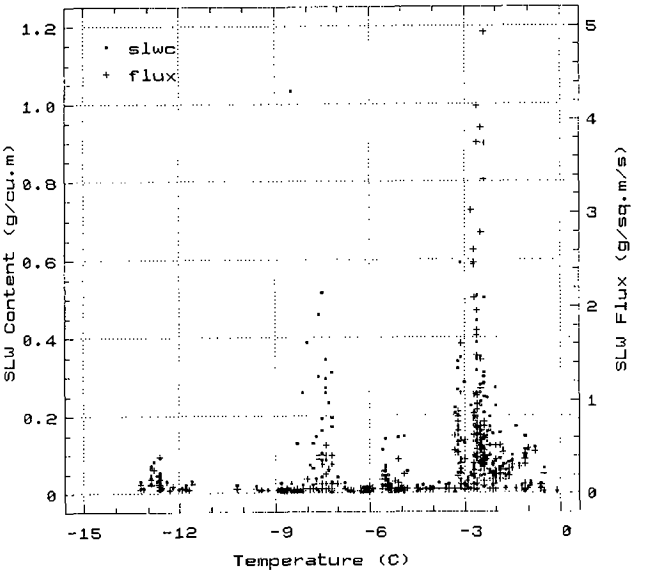

Figure 6. SLW content and flux vs. temperature during 1987 full season combined probe riming events, 5-min averages.

The SLW and precipitation data were analyzed in the following manner. A lag time of 15 minutes was employed in the riming data to attempt to relate conditions at the gage site to those at the icing station. The 15-minute lag time approximates the seasonal average wind speed of 4.5 m s^{-1}. For the full 1987 eleven-STORM sample, probe riming occurred during approximately half the 30-minute periods of measurable precipitation. Thirty-minute accumulations of precipitation and probe rime ice for each of the eleven STORM periods were compared using a linear regression analysis.

Since the Utah/NOAA project definition of a STORM includes a period of minimal activity prior to the onset of precipitation or riming, and generally continues beyond the end of any significant precipitation, a new unit of analysis called a **storm** (lower-case letters) was adopted here. In this study the **storm** is defined as the period between the first incidence of either precipitation at gage P6 or probe riming and the last incidence of either precipitation or riming. When regression analysis was performed on each **storm**, (see Table 3) an interesting pattern is observed:

-For the three **storms** (4, 3 and 9) that comprised 86% of the total seasonal SLW mass accumulation at the detector site, positive correlations of .17 to .53 were noted between precipitation amount and probe rime accumulation.

-The remaining **storms** exhibited weak negative correlations ranging from 0 to -.22, excepting overall STORM 7 which yielded: a=.39, b=-.13 and c= no precipitation at P6 for the three distinct cloud systems within STORM 7's overall duration.

TABLE 3. Correlation Coefficients of Probe Riming Rate to Precipitation Rate at Merchant Creek, Within 11 STORMS Ranked by SLW Mass Accumulation

	correl. coeff., 30 min. intervals		
STORM	STORM[1]		storm[2]
87- 4*	+0.48		+0.46
3*	+0.65		+0.53
9	+0.37		+0.17
1	-0.13		-0.17
7*#	+0.18		+0.16
		(a)	+0.39
		(b)	-0.13
		(c)	NP
2	-0.12		-0.22
11	-0.13		-0.14
8	NP		NP
6	NP		NP
5*	-0.13		-0.13
10	+0.22		0.00

1 standard project definition
2 defined as the period between the first and last occurrence of either precip at P6 or probe riming at the ice detector site
* project priority analysis cases
\# STORM 7 contains three distinct cloudy periods, labeled a, b and c
NP no measurable precipitation

Major **storms**, exemplified by numbers 4 and 3 (which produced approximately 74% of the season total probe rime mass in 1987) produced large quantities of supercooled liquid water in conjunction with precipitation rate increases. However, for the remaining 1987 **storms**, when the mid and upper barrier precipitation rate increased, the low altitude supercooled liquid water supply did not show a corresponding increase. These initial storm-scale findings challenge the notion that high precipitation rates alone necessarily signal decreased seeding opportunity because we report instances of concurrent high precipitation rates and high SLW production.

Because we have shown that both SLW production and precipitation rates vary widely between and within the various phases of significant precipitation events, it may be more instructive to assess and compare those factors at shorter (operationally meaningful) time intervals. To that end SLW flux data and precipitation rates were compared to provide indications of trends in relative precipitation efficiency. Following a comparison procedure applied by Rogers et al (1986) which used radiometer data, ice detector accretion records and precipitation data were used to develop similar relative efficiency indications for two major Utah STORMs, 85-9 and 87-4. In both cases 30-min interval data were used, matching the basic temporal resolution of the precipitation data. The ice detector accretion amounts were sums of 5-min values.

SLW flux past the ground-based detector site was calculated from the ice mass collected by the detector and adjusted for estimated collection efficiency, as described earlier. The values were expressed in kg m^{-2} h^{-1}. In these studies, precipitation rates were determined for the western slope of the Tushar Range along a 20km barrier transect from approximately 1875m elevation in the upper foothills to over 2900m in the upper watershed near the ice detector site. Thirty-minute averages of six gages (P2-P7) in 1985 and five gages (P2-P6) in 1987 were used. The gage data were converted from inches per half hour to mm h^{-1}.

The STORM 85-9 data are presented in Figures 7a and 7b. In (7a) two distinct periods of high SLW flux are clearly seen, from 1700-2200 and from 0500-0800. The earlier period of high SLW flux is not accompanied by high precipitation rates, so comparative precipitation inefficiency is inferred. In contrast, the latter period of high SLW is followed soon thereafter by a significant precipitation rate increase, so higher storm precipitation efficiency is indicated during most of that phase.

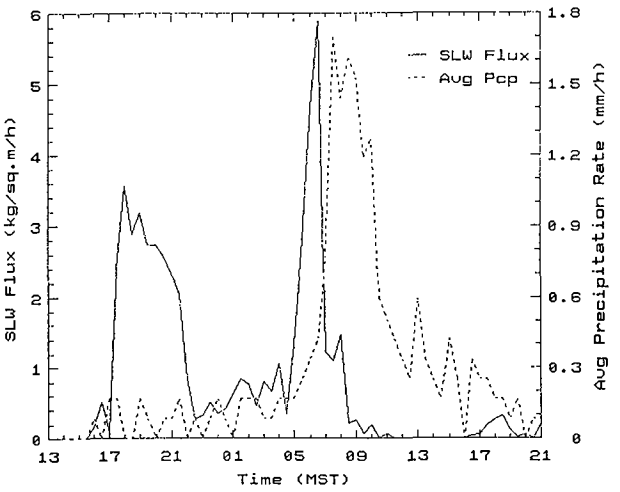

Figure 7a. Time series of 30-min Mt. Holly SLW flux and multi-gage average precipitation rate, STORM 85-9: 08-09 February 1985.

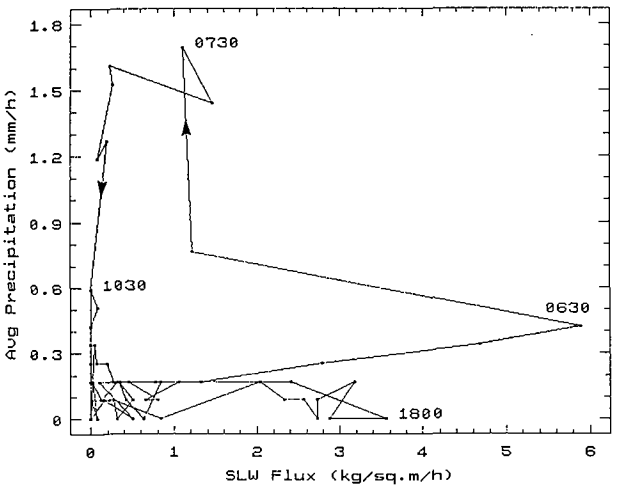

Figure 7b. Scatterplot of 30-min Mt. Holly site SLW flux and average precipitation rate, STORM 85-9: 08-09 February 1985. The points are connected to show changes in relative precipitation efficiency with time.

In (7b) the same data are presented, but as a scatterplot. When the points are connected chronologically, the plot serves to indicate trends in comparative storm efficiency and inefficiency. Our simple conceptual model of storm efficiency follows a spectrum from very high to very low precipitation efficiency. High efficiency would be characterized by high precipitation rates in conjunction with low SLW flux. Periods of low precipitation efficiency would exhibit low precipitation rates and high SLW flux. Consideration of other factors affecting precipitation enhancement potential is beyond the scope of this article. The two high SLW flux periods can be seen. The first, bracketing the label at 1800 centered in the lower portion of the plot area, shows a cluster of several half-hour periods with high SLW and low precipitation rates (inefficient precipitation production). The second high SLW flux period is initially dramatic (0630), but the points very soon migrate to the upper left portion of the plot as the precipitation increases and the SLW flux decreases, indicating a period of more efficient precipitation. Analysis of radiometer data for this storm shown in Rogers et al (1986) show the same periods of "efficiency" and "inefficiency". An important characteristic in Figure 7b is the reasonably orderly transitions between "efficient" and "inefficient" storm segments of a few hours' duration. This tendency for well-sustained temporal trends in indicated storm efficiency suggests that adequate time for recognition and assessment of potentially seedable periods exists in certain storms. This is of further significance when recalling that the storm described in Figure 7b dominated the SLW flux for the 1985 season in both the radiometer and ice detector records, producing approximately half the seasonal totals for both observation systems.

The same analysis method was applied to STORM 87-4, a well organized frontal system, which was dominant in the seasonal SLW flux data at the ice detector site. The only difference from the 85-9 study was that in 87-4 study data from the highest elevation gage (P7) were not available. In this case distinct and sustained efficient and inefficient periods were also found. The data are shown in Figures 8a and 8b. In contrast to STORM 85-9 which exhibited two SLW surges, only one dramatic period of high SLW occurred in STORM 87-4. Its onset brought modest SLW at the detector site, but precipitation across the western slope of the Tushars occurred at significant rates. After about 4 hours of relatively high precipitation rates (with average half-hourly precipitation rates peaking over 4 mm h^{-1}), dramatic prefrontal SLW increases occurred. The SLW flux peaked immediately prior to the frontal passage to nearly 15 kg m^{-2} h^{-1}, more than twice the peak value for STORM 85-9. The massive SLW flux was due to strong acceleration of the barrier component flow ahead of the surface cold front, combined with elevated SLW content. As the SLW flux was increasing, the precipitation rates trended lower than the earlier period, resulting in a 3h period of storm inefficiency representing a significant potential seeding opportunity.

Following the cold frontal passage, which was marked by thunderstorms, rapid clearing was observed across the study area. About an hour after the frontal passage, precipitation began again and was accompanied by low magnitude SLW at the detector site. This period of high precipitation efficiency lasted for about 7 hours.

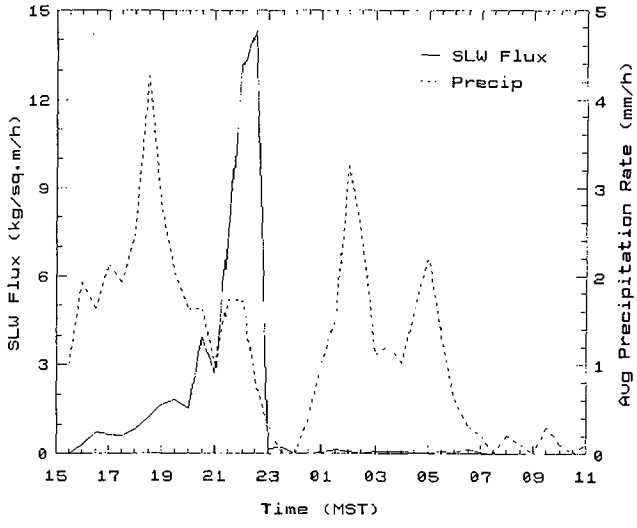

Figure 8a. Time series of 30-min Mt. Holly site SLW flux and multi-gage average precipitation rate, STORM 87-4: 13-14 February 1987.

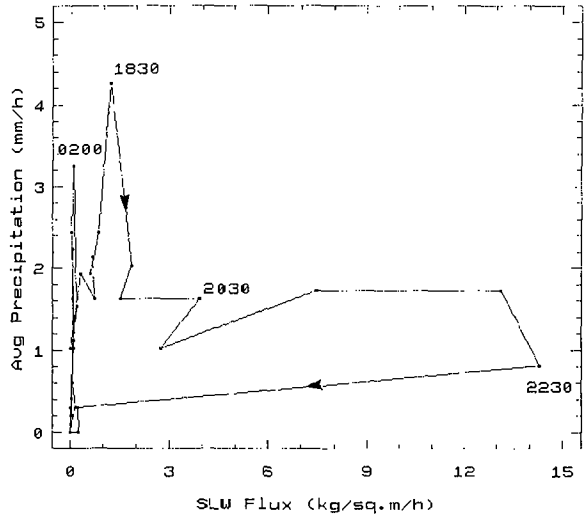

Figure 8b. Scatterplot of 30-min Mt. Holly site SLW flux and average precipitation rate, STORM 87-4: 13-14 February 1987. The points are connected to show changes in relative precipitation efficiency with time.

F. Ice Detector/Radiometer SLW Flux Comparisons

Ground-based SLW measurements in Utah and elsewhere have played a useful role in weather modification research, documenting the magnitude and frequency of low altitude SLW over mountainous terrain at altitudes where airborne measurements are not permitted. It is desirable to relate these point measurements to SLW measurements documenting the full cloud depth.

Consequently, a few preliminary comparisons between ice detector and radiometer-derived SLW flux estimates were made using Utah data. These comparisons involved the 1985 "priority analysis" cases at the STORM scale and the STORM 85-9 case at intervals as short as 30 minutes.

When STORM total SLW flux from the ice detector site was compared to the radiometer-derived estimates of full depth, barrier-wide liquid flux, the two independent systems ranked the STORMs identically. Table 4 shows the ranked totals; the dominance of STORM 85-9 is again apparent. The values are well correlated. Percentages pertain to the four-STORM sample.

TABLE 4. Ice Detector/Radiometer Flux Comparisons, STORM Scale

STORM	Ice Det Flux kg m^{-2} h^{-1}	Radiometer Flux[1] AF, 50 km width
85-9	35.44 (94.5%)	6235 (83.7%)
85-13	1.08 (2.9%)	861 (11.6%)
85-8	.86 (2.3%)	252 (3.4%)
85-11	.12 (.3%)	97 (1.3%)

[1] Corrected liquid water (AF = Acre Feet), Table III, Rogers et al. (1986)

The STORM 85-9 case was assessed at finer time intervals. Three-hour, barrier wide, (50km) radiometer liquid water volume values, calculated by Rogers et al. (1986) using 700mb rawinsonde winds, were compared with ice detector-derived flux values for corresponding time blocks. The comparison is shown in Table 5. At 3h intervals reasonable correspondence is seen, but with some apparent offsets in peak values. Those are due to the 3h averaging, especially when a dominant short-term maximum occurs near a break between intervals, but may also reflect real differences due to the altitude(s) at which the SLW was occurring. Simple correlation coefficients between the two systems' flux values are shown for 3h and 6h blocks. Improved correspondence between the two systems' data is seen at 6h, but the sample is very small.

TABLE 5. Ice Detector/Radiometer Flux Comparisons, STORM 85-9, 3 and 6-hr Scale

Rawinsonde Time (GMT)	3h avg radiom. liquid water depth (mm)	Radiom. liquid water vol (AF/50 km)		Ice det. SLW Flux (kg m^{-2} h^{-1})	
12	0.000	0.0		0.000	
15	0.000	0.0		0.000	
00 (17L)	0.273	1190.1		5.618	
			2052.6		12.921
03 (20L)	0.236	862.5		7.303	
06 (23L)	0.052	247.4		1.261	
			1513.2		3.286
09 (02L)	0.227	1265.8		2.025	
12 (05L)	0.232	1150.5		7.641	
			2345.7		10.433
15 (08L)	0.275	1195.2		2.792	
18 (11L)	0.206	312.9		0.077	
			329.6		0.542
00 (17L)	0.010	16.7		0.465	
03 (20L)	0.000	0.0		0.263	

Detector Flux vs Radiometer Volume: at 3h, r = .69, n=9
at 6h, r = .88, n=4

Comparisons were also made at 30-min intervals through the full duration of STORM 85-9, and for each of its four phases. Scatterplots of SLW flux and precipitation, drawn from the ice detector system (as shown in Figure 7b) and using radiometer data (plot not shown here) show many similarities in their respective indicated periods of precipitation inefficiency and efficiency. A more direct comparison of flux estimates involved a time series of STORM 85-9 30-min flux values from the two measurement systems through the storm, presented in Figure 9 with the four STORM phases indicated. The storm phases are described in Table 6 which appears below. The ice detector-derived values in this plot were not adjusted to account for its position downwind of the radiometer, partly because the radiometer data were obtained in varying proportions of zenith and azimuth scanning modes. Good correspondence is seen in the SLW maxima in phase I and bracketing 0600 in phase III. Poor correspondence can also be seen from mid-phase II to early phase III, and from mid-phase III through phase IV, indicating periods when the SLW was occurring above the ice detector's elevation.

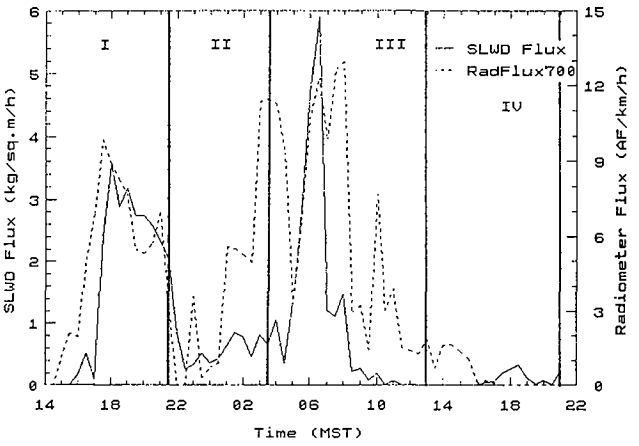

Figure 9. Time series of Mt. Holly ice detector and Merchant Valley radiometer-derived SLW flux. The project STORM phases are indicated; times are in MST.

Simple (linear) regressions were run for each of the four phases, without any time lag and with a 30-min lag applied to the detector data to account for the distance between the measurement sites. A summary is shown in Table 6. Each storm phase is described. The degree of correspondence between the mountain-top and full-depth (radiometer) flux estimates, as well as the effect of the fixed lag for advection, varies among the STORM phases. Thirty-minute data within the various phases (i.e., cloud types and synoptic patterns) show correspondence ranging from excellent (r = .91 in orographically induced altocumulus) to poor (r <.5 in shallow, dissipating layers and isolated cap clouds).

TABLE 6. Ice Detector/Radiometer SLW Flux Estimates Compared by STORM Phase, 85-9

Phase	Times (MST)	Correlation No Lag	30min Lag	Description
I	1400-2130	.771	.906	Orogr.induced/ enhanced alto cumulus layer
II	2130-0330	.490	.768	Altocu layer with embedded conv.elements
III	0330-1300	.613	.352	Immed. pre and postfrontal; synoptic scale disturbance produced meso-scale bands
IV	1300-2100	-.543	-.582	Dissip stage, decreasing precip from shallowing clouds
STORM	1400 8FEB 2100 9FEB	.636	.552	

6. CONCLUSIONS

Refinements in the ground-based supercooled liquid water system sensors, data acquisition methods and data interpretation have produced highly useful information regarding SLW characteristics for winter orographic weather modification research and operations.

Ice detector accretion data in analog form is far superior to "trip-only" records, especially for research applications. Care must be exercised in drawing conclusions from trip-only data pertaining to icing occurrence and duration, as well as in estimating SLW concentration and flux.

Comparisons of ice detector and radiometer-derived SLW flux estimates show good correspondence in many instances and informative differences in others.

Estimates of "relative precipitation efficiency" using SLW flux derived from ground-based ice detector measurements show orderly transitions between comparatively efficient and inefficient storm periods of a few hours duration. This result suggests adequate continuity for real-time recognition of, and response to, potential seeding opportunities (inefficient storm periods).

Comparisons of low-altitude SLW flux values and precipitation rates suggest that increased precipitation alone does not necessarily signal diminished augmentation potential. This suggestion must be further investigated, taking into account other factors to more objectively determine seedability.

Acknowledgements

This work was performed as one of several contracts between the State of Utah (Division of Water Resources) and a number of federal,state, university and private sector groups. In turn, the overall activities are supported by the Department of Commerce within the Utah/NOAA Cooperative Weather Modification Research Program. We are grateful for the collaboration of the many dedicated investigators within the program and the team spirit so necessary in field research programs of this type.

7. REFERENCES

Grant, L. O., and A. M. Kahan, 1974: Weather Modification for augmenting orographic precipitation. Weather and Climate Modification, Hess, Ed., 282-317.

Henderson, T.J. and M. E. Solak, 1983: Supercooled liquid water concentrations in winter orographic clouds from ground-based ice accretion measurements. J. Wea. Modif., 15, 64-70.

Hindman, E.E., 1986: Characteristics of supercooled liquid water in clouds at mountaintop sites in the Colorado Rockies. J. Climate and Appl. Meteor., 25, 1271-1279.

Lamb, D., K.W. Nielsen, H.E. Klieforth and J. Hallet, 1976: Measurement of liquid water content in winter cloud systems over the Sierra Nevada. J. Appl. Meteor., 15, 763-775.

Ranz, W. E. and J. B. Wong, 1952: Impaction of dust and smoke particles on surface and body collectors. Industrial and Engineering Chemistry, 44, 1372-1381.

Rauber, R.M. and L.O. Grant, 1986: The characteristics and distribution of cloud water over the mountains of northern Colorado during wintertime storms. Part II: spatial distribution and microphysical characteristics. J. Clim. and Appl. Meteor., 25, 489-504.

Rogers, D.C., R.M. Rauber, L.O. Grant, 1986: Studies of wintertime storms over the Tushar Mountains of Utah. Report by Colo. State Univ. Ft. Collins to Utah Division of Water Resources, 50 pp.

Sassen, K., 1985: Supercooled liquid water in winter storms, 1985. Preliminary climatology from remote sensing observation. J. Wea. Modif., 17, 30-35.

Snider, J.B. and D. Rottner, 1982: The use of microwave radiometry to determine a cloud seeding opportunity. J. Appl. Meteor., 21, 1286-1291.

Solak, M.E., T.J. Henderson and R.B. Allan, 1984: Final report - data collection and analysis, volume three - ground based measurement systems, SCPP. Report by Atmospherics Inc. submitted to Bureau of Reclam., 70 pp.

Thompson, J.P. and A.B. Super, 1987: Wintertime supercooled liquid water flux over the Grand Mesa, Colorado. J. Wea. Modif., 19, 92-98.